Supporting information

The calculate the absorbed photocurrent density of the photoelectrode: J_{abs} is defined as the photocurrent density generated when the photoelectrode converts 100% of the absorbed photon energy into electrons and holes, representing the theoretical relationship that the absorbed photons completely convert the photocurrent. $P_{abs}(\lambda)$ ($mW/(cm^2 \cdot nm)$) is integrated with the wavelength λ to obtain the total power (mW/cm^2), that is, the power actually absorbed by the photoelectrode, which is then converted into the photocurrent J_{abs} according to equation (11):

$$J_{abs}(\frac{mA}{cm^2}) = \int_{\lambda_1}^{\lambda_2} \frac{\lambda(nm)}{1240(V \cdot nm)} \times \frac{P_{abs}(\lambda)}{10}(\frac{mW}{cm^2 \cdot nm})d\lambda \tag{11}$$

In addition, Fig. S7 can be obtained from the UV/Vis absorption spectrum, which is the cut-off wavelength diagram of the photoelectrode light absorption under AM 1.5 G simulated sunlight illumination, and the arrow indicates the intrinsic absorption of the photoelectrode.

In the previous experiment, we controlled the grain size by hydrothermal time and temperature. The $NaNbO_3$ prepared by hydrothermal method was orthorhombic phase. As shown in the Fig. S11a-c, it can be clearly observed that when the hydrothermal time is 4 h, 6 h and 10 h, the grain size is ~0.5 μm, ~1 μm and ~2 μm respectively. The grain size increases with the increase of hydrothermal time. According to the hydrothermal temperature gradient experiment (Fig. S11d-c), with the increase of hydrothermal temperature, the grains gradually grow and become more complete, showing a cube-shaped structure.

Using samples with different grain sizes synthesized in previous experiments, we compared the effects of different grain sizes on pyro-photo-electric catalytic properties. As shown in the Fig. S12, under the stimulation of light and thermal cycle, when the grain size of the sample is ~1 μm, the current density reaches 0.38 mA/cm^2 at 1.23 V_{RHE}, higher than ~0.5 μm and ~2 μm samples. This indicates that when the grain size of the sample is ~1 μm has better pyro-photo-electric catalytic properties. We speculate that the reason may be the difference of spontaneous polarization intensity[60].

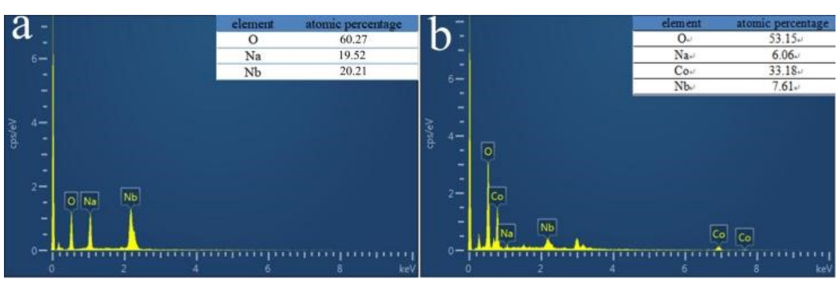

Fig. S1 EDS elemental analysis spectrum. (a) $NaNbO_3$ photoanode; (b) $NaNbO_3/Co(OH)_2$ composite electrode

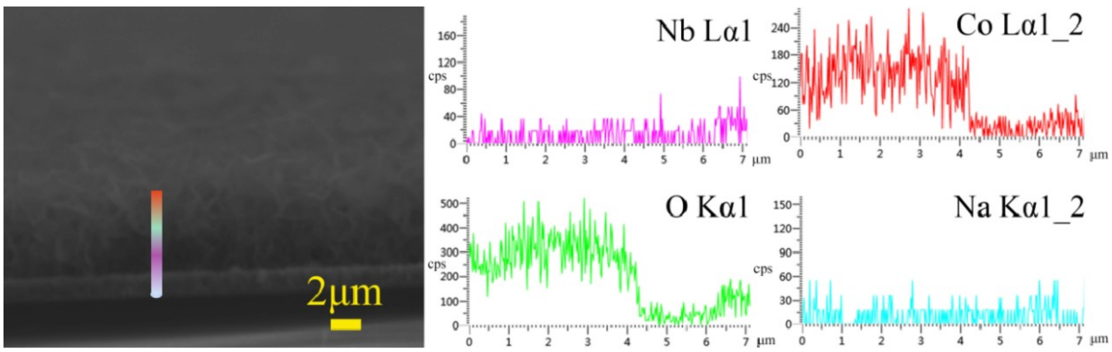

Fig.S2 Cross-sectional SEM image of $NaNbO_3/Co(OH)_2$ composite electrode, showing the EDS line scan at which the atom distribution

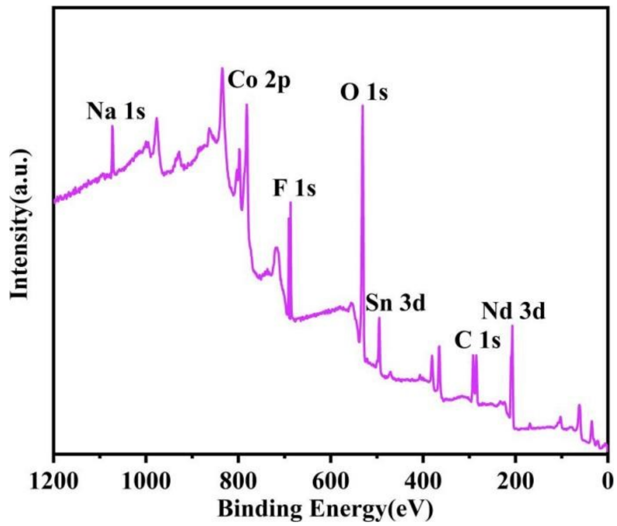

Fig.S3 XPS spectra of survey

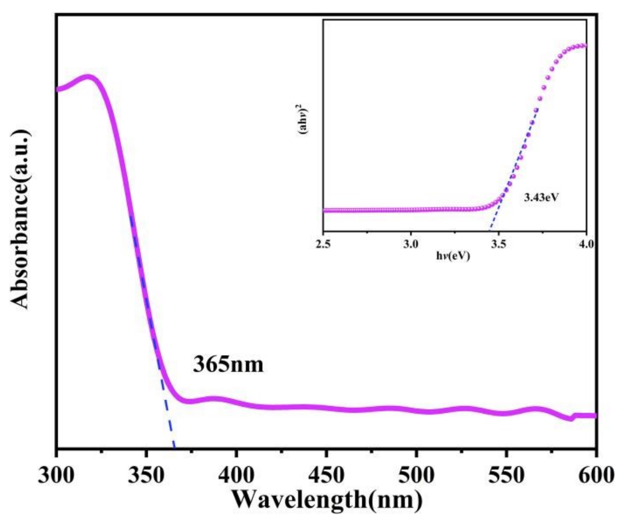

Fig.S4 UV-visible absorption spectrum of $NaNbO_3$, the inset is $(\alpha h\nu)^2$ versus photon energy (hν) curve

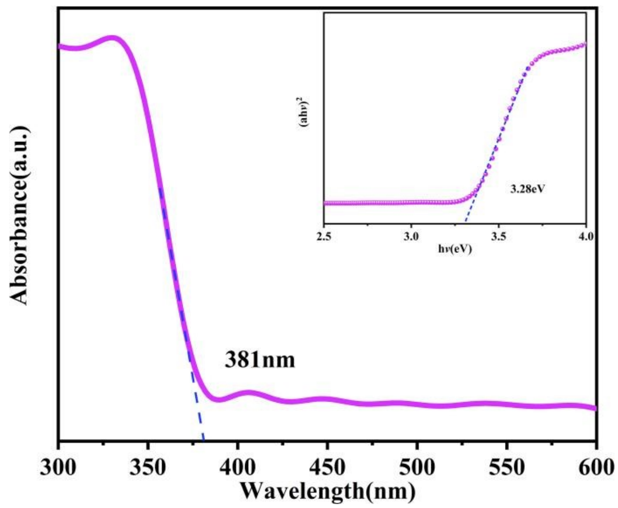

Fig.S5 UV-visible absorption spectrum of $NaNbO_3/Co(OH)_2$, the inset is $(\alpha h\nu)^2$ versus photon energy (hν) curve

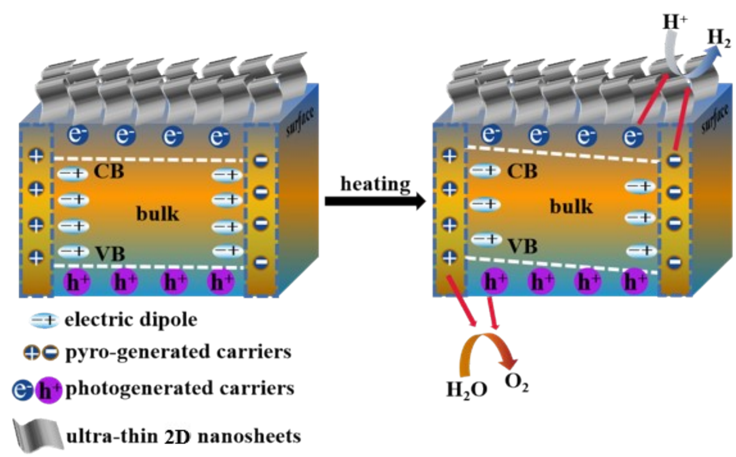

Fig. S6 The mechanism of pyro-photo-electric catalysis process

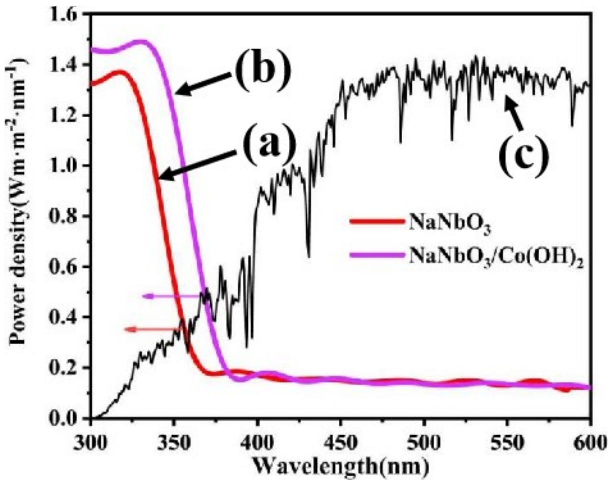

Fig.S7 The light absorption cut-off wavelength diagram of $NaNbO_3$ electrode and $NaNbO_3/Co(OH)_2$ composite electrode under AM 1.5G simulated sunlight illumination (100 mW/cm^2); (a) $NaNbO_3$ electrode; (b) $NaNbO_3/Co(OH)_2$ composite electrode; (c) AM 1.5G simulated sunlight illumination power density

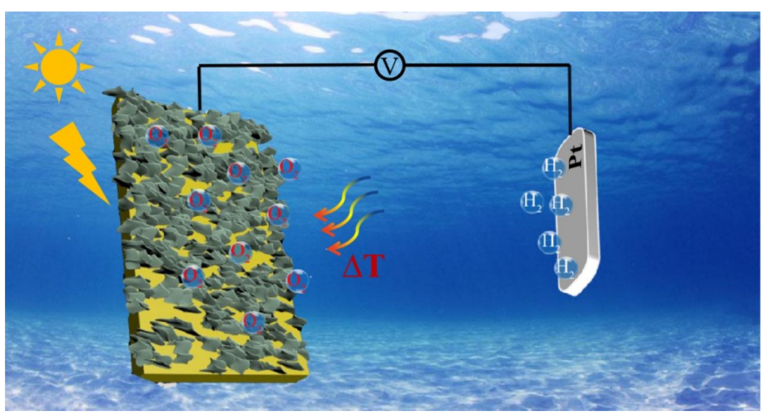

Fig. S8 Schematic diagram of synergistic water splitting by pyroelectric and photoelectrochemical catalysis

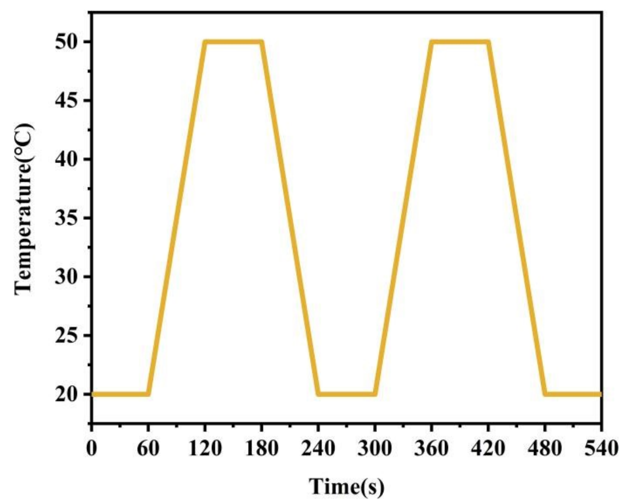

Fig. S9 The ideal temperature curve for cold-hot thermal cycles

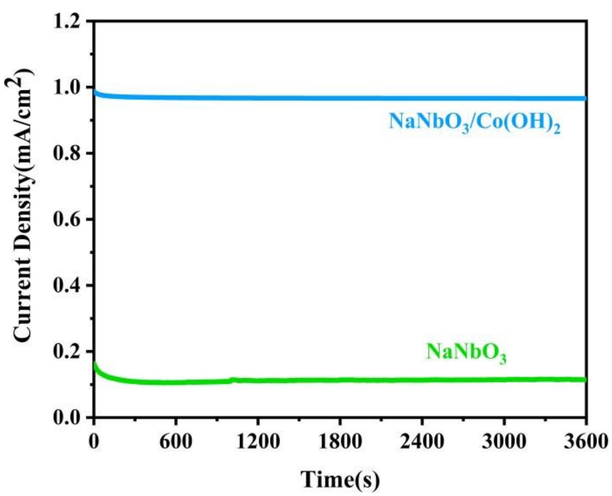

Fig. S10 Steady-state current curves of $NaNbO_3$ electrode and $NaNbO_3/Co(OH)_2$ composite electrode measured in 1.0 M Na_2SO_4 (pH=6.8) electrolyte under consistent one sun illumination for 3600 s

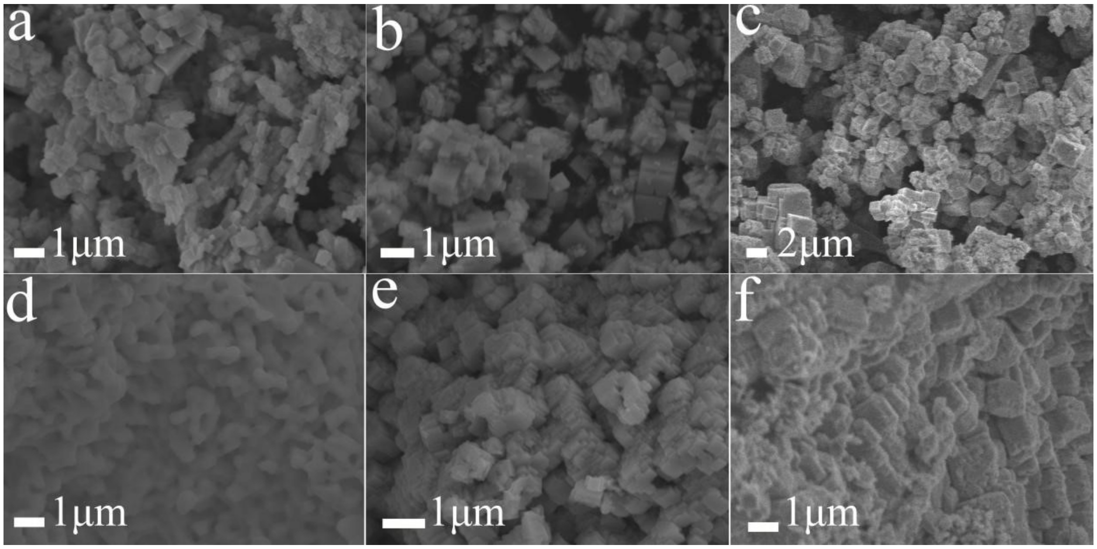

Fig. S11 The $NaNbO_3$ synthesized at different hydrothermal time and temperature; (a) 160 ℃-4 h; (b) 160 ℃-6 h; (c) 160 ℃-10 h; (d) 120 ℃-8 h; (e) 140 ℃-8 h; (f) 180 ℃-8 h

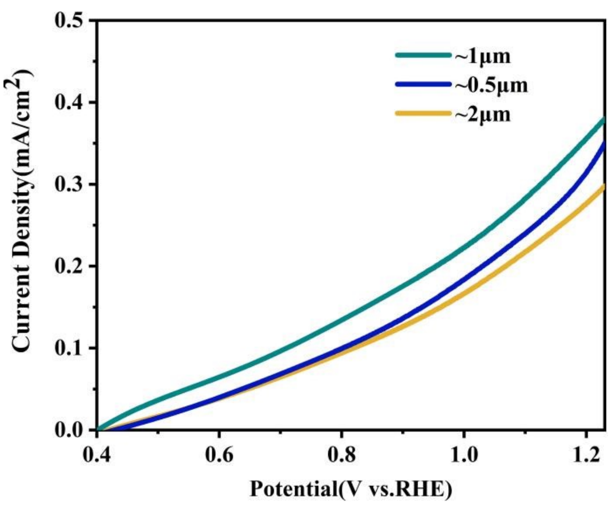

Fig. S12 The I-V curves of $NaNbO_3$ samples with different grain sizes (Under the light + △T)

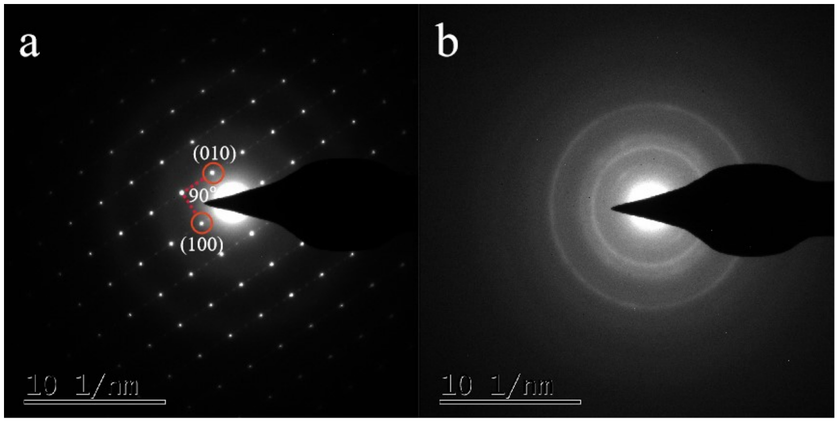

Fig. S13 The SEAD of $NaNbO_3$ and $Co(OH)_2$; (a) $NaNbO_3$; (b) $Co(OH)_2$

Tab. S1 Flat band potential (V_{fb}) and donor density (N_d) of electrodes deduced from Mott-Schottky

Sample	$NaNbO_3$			$NaNbO_3/Co(OH)_2$		
conditions	light	ΔT	light + ΔT	light	ΔT	light + ΔT
V_{fb} (V) Vs. RHE	-0.01	0.1	-0.26	-0.21	-0.06	-0.36
N_d (*$10^{17}cm^{-3}$)	7.7	6.9	10	14.1	10.2	20.6

Tab. S2 the comparison of pyro-photo-electric catalytic properties of other composites

Materials	pyro-photo-electric catalytic properties	Publishing year
$BaTiO_{3-X}$-5%[61]	0.77 mA/cm^2	2022
$Ba_{0.7}Sr_{0.3}TiO_{3-X}$[62]	0.92 mA/cm^2	2022
$K_xNa_{1-x}NbO_3$[63]	0.528 mA/cm^2	2022
$NaNbO_3/Co(OH)_2$	1.68 mA/cm^2	